A Simple Alternative to the Expression of Finite Warburg Diffusion Impedance in Porous Electrodes by Considering Oxygen Consumption Along the Air Channel

Julia Mainka, Gaël Maranzana, Jérôme Dillet, Sophie Didierjean, Olivier Lottin

A simple alternative to the expression of finite Warburg diffusion impedance in porous electrodes by considering oxygen consumption along the air channel

J. Mainka, G. Maranzana, J. Dillet, S. Didierjean, O. Lottin

LEMTA, Nancy University - CNRS, 2 avenue de la Fôret de Haye BP160, 54504 Vandoeuvre les Nancy Cedex, France.

The classical expression of the finite Warburg element used for analysing electrochemical impedance spectroscopy (EIS) spectra is obtained assuming that the reaction occurs at the electrode/membrane interface and that the oxygen concentration at the gas channel/gas diffusion layer interface is constant. An alternative to this expression is proposed: it takes into account the variation in oxygen concentration along the gas channel due to the oxygen-reduction reaction (ORR). This pseudo-2D approach is well suited for investigating mass transfer limitations in the fuel cell membrane-electrode assemblies (MEA). Simple numerical applications starting from data already published by different authors show that with this new expression, conclusions about the mass transfer limiting layer and its main characteristics can be significantly modified. This improvement to the usual Warburg impedance could contribute to a better understanding of mass transfer limitation in fuel cells and eventually, to the design of MEAs in which diffusion losses are minimal.

Introduction

Fuel cell development has made considerable progress in recent years, so that their incorporation in mobile and stationary power applications becomes a realistic aim for the near future. Among the different categories of fuel cells (depending on the fuel and on the type of electrolyte), proton exchange membrane fuel cells (PEMFC) are very promising because of their moderate operating conditions (temperatures < 100 °C, gas pressures from 1 to 3 atm (1)). Fed by pure hydrogen and air, they do not emit any greenhouse gases.

Fuel cells must be able to operate at high current densities with a satisfying efficiency and reasonable gas consumption. Under these conditions, the slow oxygen diffusion to the cathode reaction sites is a significant impediment, which has a direct influence on the oxygen reduction reaction (ORR) kinetics: for instance, various studies highlight the role of the gas diffusion layer in oxygen mass transport limitations in PEMFC (2,3). Hence, there is a need for mass transfer studies pointing out clearly the origin of the oxygen diffusion limitations, for which EIS can be of great interest besides of being a powerful technique for investigating electrochemical reaction kinetics in the porous electrodes.

The first one-dimensional steady-state diffusion model proposed by Springer et al. (4) made it possible to analyse fuel cells performance dependence on water management. Since, many improvements have been brought to the theoretical models. Most of them

focus on charge and mass transfer dynamics in the cathode active layer (5-7). Eikerling and Kornyshev (6) even developed a model describing potential and concentration gradients through the active layer in the direction perpendicular to the electrode surface. In parallel, EIS allows to investigate the different processes occurring in PEMFCs (8) and to analyse in situ fuel cells behaviour (9,10). One of the most common expressions of diffusion impedance used in fuel cell equivalent circuits is the finite Warburg element (11). It is based on simple assumptions: Fick's diffusion of oxygen, surface reaction, and a constant concentration at the gas channel boundary of the diffusion medium. The resulting expression of the diffusion impedance yields surprisingly good results. However, in order to improve this model, a decreasing oxygen concentration profile along the gas channel can be used as a boundary condition. This does not change radically the expression of the diffusion impedance, but it is a first step for obtaining a more accurate mass transfer model.

Theoretical Model

Before accessing the active reaction sites, air and hydrogen have to flow through different media: the bipolar plates ensuring the gas supply via the flow-field channels, the gas diffusion layers (GDL) homogenising the gas propagation over the electrodes, and the catalyst layers consisting of a porous mixture of carbon powder and catalyst particles embedded in the electrolyte. Gases have to flow through their pores and the electrochemical reactions occur on (or in) the solid phase. Mass transfer models should take into account as well as possible the geometrical characteristics of these successive media but actually, the finite Warburg element describes only gas diffusion through a homogeneous medium.

Mass transfer model

According to the majority of the authors (5,6,12), the oxygen reduction reaction is the limiting factor for the energy conversion process in PEMFC and on top of that, the access of oxygen to the reaction sites remains problematic, due to the (possible) presence of liquid water in the MEA and to the low oxygen partial pressure when the fuel cell is fed by air (1). On the other hand, since the cathode is the place of water production, the ionic resistance of the well-hydrated polymer can be neglected. As a consequence, the main hypotheses of the one-dimensional cathode model, where oxygen transport occurs only by diffusion are:

- The fuel cell is isotherm and isobar.
- Ohmic drops in the active layer and in the GDL are neglected due to their high ionic and electronic conductivity.
- Mass transfer of O_2 and H_2O is assumed to occur only by diffusion in the pores of the active layer and the GDL.
- There is no H_2O diffusion through the agglomerates.

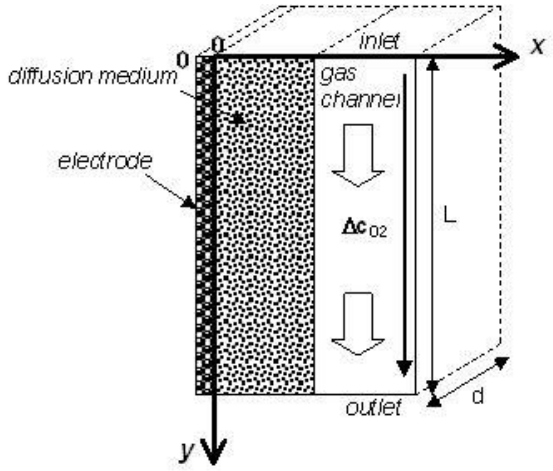

Figure 1. Schematic representation of the pseudo 2D diffusion model. Oxygen concentration variation in the channel is taken into account for mass transfer modelling.

These are usual assumptions for one-dimensional mass transfer modelling in fuel cells. In order to obtain a pseudo-2D model (Figure 1), which takes into account oxygen concentration variation along the gas channel, three more hypotheses are made:

- Mass transfer limitations in the gas channel are neglected.
- Time variations of the oxygen concentration in the channel are neglected.
- The Tafel slope b is constant *b*etween the inlet and the outlet of the air channel.

The electrode surface is given by $L \times d$; the gases flow along the channel length L.

Usually, it is preferable to use a Butler-Volmer formalism to describe oxygen reduction kinetics (13) but for sufficiently high current densities and in steady state, the activation overpotential follows a Tafel law of the form:

$$\eta_{act} = b \ln \frac{j_f(y) c_{02}^0}{j_0 c_{02}(x=0,y)} \qquad [1]$$

In equation [1], the faradaic current density $j_f\ (y)$ and the oxygen concentration $c_{O2}\ (x,y)$ vary along the gas channel, i.e. as functions of the y coordinate (Figure 1). The cell average current density J is given by:

$$J = \frac{1}{L} \int_0^L j_f dy \qquad [2]$$

It is worth mentioning that by convention, the activation overpotential as well as the faradaic current density at the cathode side are usually negative. However, for convenience their absolute values are considered in the following: $j_f(y,t) > 0$.

Under the conditions mentioned above, the molar fluxes of oxygen and water in the channel depend also on their *y*-position. Thus, the molar flux of oxygen $N_{O2}(y)$ corresponds to that at the inlet of the gas channel minus the flux consumed at the cathode:

$$N_{02}\left(y\right) = N_{02}^{in} - \frac{d\int_{0}^{y} j_f dy}{4F} \qquad [3]$$

Supposing that all water produced by the fuel cell remains in the air channel, it comes:

$$N_{H20}\left(y\right) = N_{H20}^{in} + \frac{d\int_{0}^{y} j_f dy}{2F} \qquad [4]$$

The fuel cell being fed by air, the oxygen molar ratio at the GDL/gas channel interface as a function of y is given by:

$$y_{02}\left(y\right) = \frac{N_{02}\left(y\right)}{N_{02}\left(y\right) + N_{N2} + N_{H20}\left(y\right)} = \frac{N_{02}^{in} - \frac{d\int_{0}^{y} j_f dy}{4F}}{N_{02}^{in} - \frac{d\int_{0}^{y} j_f dy}{4F} + N_{N2} + N_{H20}^{in} + \frac{d\int_{0}^{y} j_f dy}{2F}}$$

And considering that $N_{N2} = 4N_{O2}^{in}$, the above equation simplifies into:

$$y_{O2}(y) = \frac{S_{02} - \frac{d\int_{0}^{y} j_f dy}{I}}{5S_{02}\left(1+H\right) + \frac{d\int_{0}^{y} j_f dy}{I}}. \qquad [5]$$

Where $S_{02} = \frac{N_{02}^{in}}{I/4F}$ is the oxygen stoichiometry and $H = \frac{N_{H20}^{in}}{N_{02}^{in} + N_{N2}}$ the absolute humidity at the air inlet. Thus, the mean oxygen concentration at the GDL/channel interface is $\left\langle c_{02}\left(x=\delta, y\right)\right\rangle$ assumed equal to its value in steady-state (time variations are neglected):

$$c_{02}\left(x=\delta,y\right)=\frac{P}{RT}y_{O2}(y)$$
$$=\frac{P}{RT}\frac{S_{02}-\frac{d\int_0^y j_f dy}{I}}{5S_{02}\left(1+H\right)+\frac{d\int_0^y j_f dy}{I}}. \quad [6]$$

Neglecting the integral in the denominator of [6], it can finally be approached by:

$$c_{02}\left(x=\delta,y\right)=\frac{S_{02}-\frac{d\int_0^y j_f dy}{I}}{S_{02}\left(1+H\right)}c_{02}^0. \quad [7]$$

With $c_{O2}^0=c_{O2}\left(x=\delta,0\right)$. According to the previous hypotheses, mass transport of oxygen through the pores of the GDL and those of the electrode is described by Stefan-Maxwell equations (1,14,15). However, since the binary diffusion coefficients of O_2/H_2O and O_2/N_2 are close to each other, it seems reasonable to use Fick's 1st law. Assuming that the electrochemical reaction takes place only at the active layer/membrane interface (x = 0), the 1st Fick's law can be written:

$$N_{O2}\left(y\right)=-D_{eff}\left.\frac{\partial c_{O2}}{\partial x}\right|_{\substack{x=0\\y}}. \quad [8]$$

The gas diffusion and active layers being porous, it is necessary to use an effective diffusion coefficient D_{eff} (16,17) taking into account their porosity ε and possibly, the presence of Knudsen diffusion (1,17). The most common expressions obey Archie's law (18,19):

$$D_{eff}=D\varepsilon^m \quad [9]$$

Where m is an exponent varying between 1.5 and 4. In the case of a 3D medium, there is a wide consensus for using m = 3/2, which corresponds to the differential effective medium approximation introduced by Bruggeman (19,20). m = 3/2 is probably appropriate for the active layers, in which the orientation of the solid phase does not follow a privileged direction (although this is not true in the agglomerate models using a cylindrical description). In the gas diffusion layers however, the solid phase can be considered as two-dimensional since the carbon fibres are mainly parallel to the electrodes. In this case, the result of the differential effective medium theory is m = 2 (19). In a liquid, the diffusion is governed by shocks between particles and D corresponds to the molecular diffusion coefficient D_{mol}. In a gas, two cases have to be distinguished depending on the values of the pore size and of the molecules mean free path λ (14):

$$\lambda = \frac{RT}{\pi\sqrt{2}PN_A\sigma^2} \qquad [10]$$

Where N_A is the Avogadro number and σ the mean molecule diameter. If the mean free path is much smaller than the pore size inter-molecule collisions govern the diffusion process and $D = D_{mol}$. If the mean free path is of the same range as the pore size ($\lambda \approx d_{pore}$) molecule collisions with the pore wall become significant and the Knudsen diffusion must be considered. This is not the case in the GDL where the typical pore size is between 20 and 50 μm (21). On the other hand, Kong et al. (22) showed that in most of the active layers, the pore size is between 30 and 60 nm. Therefore, the Knudsen diffusion has to be taken into account. Since the mean free path of the gas molecules is of the same order of magnitude as the pore size, there exist various more or less sophisticated expressions combining D^K and D_{mol} for estimating the diffusion coefficient D. One of the most simple is the *Bosanquet formula* $\frac{1}{D} = \frac{1}{D_{mol}} + \frac{1}{D^K}$ the Knudsen diffusion coefficient of species i D_i^K can be expressed by $D_i^K = \frac{1}{3} d_{pore}\sqrt{\frac{8RT}{\pi M_i}}$.

DC solution

In steady-state conditions, c_{O2} and N_i (with i = O_2, N_2, H_2O), as well as j_f and η_{act} are constant in time. As the different species are neither consumed nor produced in the diffusion layers, their molar fluxes depend only on the y position. Nitrogen being inert, its flux is null while oxygen and water fluxes can be expressed by $j_f(y)$:

$$N_{N2}(y) = 0, \qquad N_{O2}(y) = -\frac{j_f(y)}{4F}, \qquad N_{H2O}(y) = \frac{j_f(y)}{2F} \qquad [11]$$

Solving the two Fick's diffusion equations in steady-state, knowing the oxygen concentration at the channel/diffusion layer interface [7] yields an expression for $c_{O2}(x,y)$. Fick's 2nd law in steady-state conditions is given by:

$$0 = D_{eff}\frac{\partial^2 c_{02}}{\partial x^2} . \qquad [12]$$

Using equation [11] relating j_f and the molar oxygen flux, the 1st Fick's law [8] gives:

$$D_{eff}\left.\frac{\partial c_{O2}}{\partial x}\right|_{\substack{x=0 \\ y}} = \frac{j_f(y)}{4F}. \qquad [13]$$

This leads to the following expression for oxygen concentration in steady-state:

$$c_{02}(x,y) = \frac{IS_{02} - d\int_0^y j_f dy}{IS_{02}(1+H)}c_{02}^0 - \frac{j_f\delta}{4FD_{eff}}\left(1-\frac{x}{\delta}\right) . \qquad [14]$$

For comparison, the oxygen concentration in the classical 1D model is expressed by:

$$c_{02}(x) = c_{02}^{0} - \frac{J\delta}{4FD_{eff}}\left(1 - \frac{x}{\delta}\right) . \qquad [15]$$

The difference between [14] and [15] lies in the oxygen concentration at the gas channel boundary. In the one-dimensional model, it is constant over the electrode surface, whereas in the two-dimensional model it varies between the gas inlet and the outlet.

AC solution

When a small sinusoidal perturbation $\Delta j_f\,(y,t)$ is added to the mean (DC) current density $\langle j_f(y)\rangle_t$, the oxygen concentration c_{O2} fluctuates around its steady-state value with the same frequency. Solutions for the current density and the concentration must obey the following conditions:

$$\Delta c_{02}(x,y,t) = c_{02}(x,y,t) - \langle c_{02}(x,y)\rangle_t = \Delta\bar{c}_{02}(x,y)\exp(iwt) \qquad [16]$$

$$\Delta j_f(y,t) = j_f(y,t) - \langle j_f(y)\rangle_t = \Delta\bar{j}_f(y)\exp(iwt). \qquad [17]$$

And the time-averaged values of the oxygen concentration $\langle c_{O2}(x,y)\rangle_t$ and of the current density $\langle j_f(y)\rangle_t$ correspond to the steady-state solution [14]:

$$\langle c_{02}(x,y)\rangle_t = \frac{IS_{02} - d\int_0^y \langle j_f(y)\rangle_t\, dy}{IS_{02}(1+H)} c_{02}^{0} - \frac{\langle j_f(y)\rangle_t\,\delta}{4FD_{eff}}\left(1 - \frac{x}{\delta}\right). \qquad [18]$$

Thus, in boundary conditions [7] and [13], the current density is replaced by its time-averaged expression $\langle j_f(y)\rangle_t$. Fick's 2nd law in AC conditions is given by:

$$\frac{\partial c_{02}}{\partial t} = D_{eff}\frac{\partial^2 c_{02}}{\partial x^2} \qquad [19]$$

Resolving this system of partial differential equations yields the following expression for $c_{O2}(x,y,t)$:

$$c_{02}(x,y,t) = \mathrm{Re}\left(-\frac{\Delta\bar{j}_f(y)}{4F\sqrt{jwD_{eff}}} \frac{\sinh\left(\sqrt{\frac{jw(\delta-x)^2}{D_{eff}}}\right)}{\cosh\left(\sqrt{\frac{jw\delta^2}{D_{eff}}}\right)} e^{iwt} \right) + \frac{IS_{02} - d\int_0^y \left\langle j_f(y)\right\rangle_t dy}{IS_{02}(1+H)} c_{02}^0 - \frac{\left\langle j_f(y)\right\rangle_t \delta}{4FD_{eff}}\left(1-\frac{x}{\delta}\right)$$

[20]

At $x = 0$, the variation in oxygen concentration $\Delta c_{O2}(x = 0,y,t)$ is given by:

$$\Delta c_{02}(x=0,y,t) = -\frac{\Delta\bar{j}_f(y)}{4F\sqrt{jwD_{eff}}} \tanh\left(\sqrt{\frac{jw\delta^2}{D_{eff}}}\right) \cdot e^{iwt}, \quad [21]$$

which makes it possible to express the faradaic impedance, defined as:

$$Z_f = \frac{\Delta\bar{\eta}_{act}}{\Delta\bar{j}_f} = \frac{\partial\bar{\eta}_{act}}{\partial\bar{j}_f} + \frac{\partial\bar{\eta}_{act}}{\partial\bar{c}_{O2}} \frac{\partial\bar{c}_{O2}}{\partial\bar{j}_f}\bigg|_{x=0}. \quad [22]$$

The first term $\frac{\partial\bar{\eta}_{act}}{\partial\bar{j}_f}$ is the charge transfer resistance R_{ct}, which can be obtained by deriving the Tafel law [1]:

$$R_{tc}(y) = \frac{b}{\left\langle j_f(y)\right\rangle_t}, \text{ in Acm}^2. \quad [23]$$

The second term $\frac{\partial\bar{\eta}_{act}}{\partial\bar{c}_{O2}} \frac{\partial\bar{c}_{O2}}{\partial\bar{j}_f}\bigg|_{x=0}$ corresponds to the mass transfer impedance Z_{co2}. Electrochemical impedance spectroscopy analyses small perturbations around the steady-state values, so that $\frac{\partial\bar{c}_{O2}}{\partial\bar{j}_f} \approx \frac{\Delta\bar{c}_{O2}}{\Delta\bar{j}_f}$. Therefore, the mass transfer impedance can be calculated with [21] and [17], which yields:

$$Z_{cO2}(y) = b \frac{\tanh\left(\sqrt{\frac{jw\delta^2}{D_{eff}}}\right)}{4F\left\langle c_{02}(x=0,y)\right\rangle_t \sqrt{iwD_{eff}}}. \quad [24]$$

The oxygen concentration at $x = 0$ can be obtained with [18]. The expression of the diffusion impedance [24] can also be written:

$$Z_{co2}(y) = R_d^{2D} \frac{\tanh\left(\sqrt{iw\tau_d}\right)}{\sqrt{iw\tau_d}}, \quad [25]$$

with the low frequency limit R_d^{2D}

$$R_d^{2D} = \frac{b\delta}{4FD_{eff}\left\langle c_{02}(x=0,y)\right\rangle_t} \quad [26]$$

and the characteristic diffusion time τ_d

$$\tau_d = \frac{\delta^2}{D_{eff}}. \quad [27]$$

At the first sight the expression of the pseudo-2D diffusion impedance is identical to a classical finite Warburg element (11):

$$Z_W = R_d^{1D}\frac{\tanh\left(\sqrt{iw\tau_d}\right)}{\sqrt{iw\tau_d}}, \quad [28]$$

with

$$R_d^{1D} = \frac{b\delta}{4FD_{eff}\left\langle c_{02}(x=0)\right\rangle_t}. \quad [29]$$

The characteristic diffusion time τ_d is also the same as in the pseudo 2D model [27]. Actually, the difference lies in the expression of the low frequency limit $R_d^{1D/2D}$: in the pseudo 2D model [26] the oxygen concentration $\left\langle c_{02}(x=0,y)\right\rangle_t$ depends on the y position, which should improve the precision of parameter estimation starting from the global diffusion impedance as well as from its local values along the cell.

Results and discussion

Applied to actual fuel cell systems, the pseudo-2D diffusion model gives access to the global and local mass transfer characteristics under specified working conditions. It is used to analyse data taken from the literature (15,23) in order to open a discussion about its accuracy and interest.

Analysis of local mass transfer

It can be useful to assess the local gas diffusion conditions in a given MEA in order to determine the optimal operating parameters. From [26] and [18], an explicit expression for the diffusion resistance $R_d^{2D}(y)$ can be obtained. Calculating the R_d^{2D} profile between the gas inlet and the gas outlet reflects the local mass transfer dynamics, which affects in turn the oxygen reduction kinetics:

$$R_d^{2D} = \frac{b\delta}{4FD_{eff}\dfrac{IS_{O2} - d\int_0^y \left\langle j_f(y)\right\rangle_t dy}{IS_{O2}(1+H)}c_{O2}^0 - \left\langle j_f(y)\right\rangle_t \delta}. \quad [30]$$

The results illustrated below are deduced from data published by *Bultel et al.* (15). They correspond to a H_2/air PEMFC operating at 60 °C and with an inlet relative humidity of about 90%. The characteristics of the gas diffusion layer and the main operating conditions are summarized in table I.

Table I: Values of the parameters used for mass transfer kinetic analysis (15).

T_{cell} [°C]	60
H [-]	0.9
p [atm]	1
S_{O2}[1] [-]	2 (if not mentioned otherwise)
$A_{electrode}$ [cm^2]	0.5
L[1] [cm]	1
d[1] [cm]	0.5
δ_{GDL} [µm]	500 (if not mentionend otherwise)
ε_{GDL}	0.2
$D_{eff_{O2,H2O}}^{GDL}$ [$m^2\ s^{-1}$]	3.98 10^{-5} x ε_{GDL}^2
b [$V\ dec^{-1}$]	0.22
I [A]	0.25

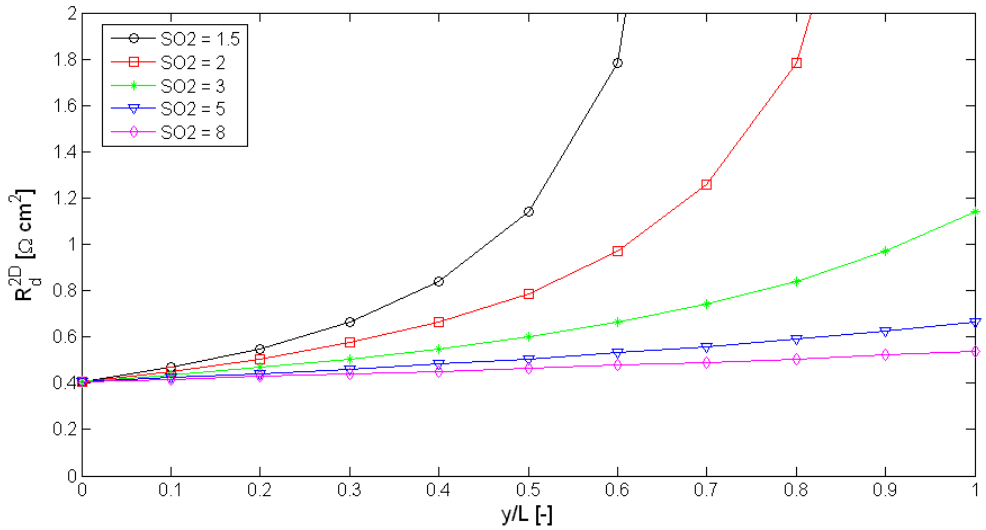

Figure 2. $R_d^{2D}(y)$ profiles between the air inlet and the air outlet for different air stoichiometries. The curves tend toward infinity for $S_{O2} < 1.93$ according to eq. [31] and to the values of the parameters given in table I.

Assuming a constant local current density $j_f = I / dL$, the integral in [30] allows to obtain a numerical values of $R_d^{2D}(y)$ for each position *y*. Fig.2 shows the modelled profiles of $R_d^{2D}(y)$ under the operating conditions of table 1 and for air stoichiometries varying between 1.5 an 8. The increase in $R_d^{2D}(y)$ from the air inlet to the air outlet depends on the air stoichiometry. There is a critical value of the air stoichiometry $S_{O2}^{crit}(\delta)$ -depending on the diffusion medium thickness δ- for which no oxygen can access to the active sites beyond a limiting length y_{lim}. As a consequence, for *y*

approaching y_{lim}, R_d^{2D} tends toward infinity. $S_{O2}^{crit}(\delta)$ is defined as the stoichiometry factor for which the oxygen concentration at the electrode/membrane interface at the gas channel outlet $c_{O2}(x=0, y=L)$ is null. In steady-state conditions and from [14], it comes:

$$S_{O2}^{crit} = \frac{c_{02}^0}{c_{02}^0 - \frac{J\delta}{4FD_{eff}}(1+H)} \quad [31]$$

In the example of Figure 2, $S_{O2}^{crit}(\delta)$ is about 1.93 and for S_{O2} = 1.5, there is no oxygen reaching the electrode/membrane interface beyond y_{lim}/L = 0.78. The analysis of $R_d^{2D}(y)$ profiles makes it possible to determine in which conditions the diffusion impedance can be described by a one-dimensional model (when, for instance, the maximum relative variation over the electrode length $\Delta R_d^{2D}(L) = \left| \frac{R_d^{2D}(L) - R_d^{2D}(0)}{R_d^{2D}(0)} \right|$ is below 10%). For this example (15), a one-dimensional behaviour would be achieved only for air stoichiometries S_{O2} above 11.

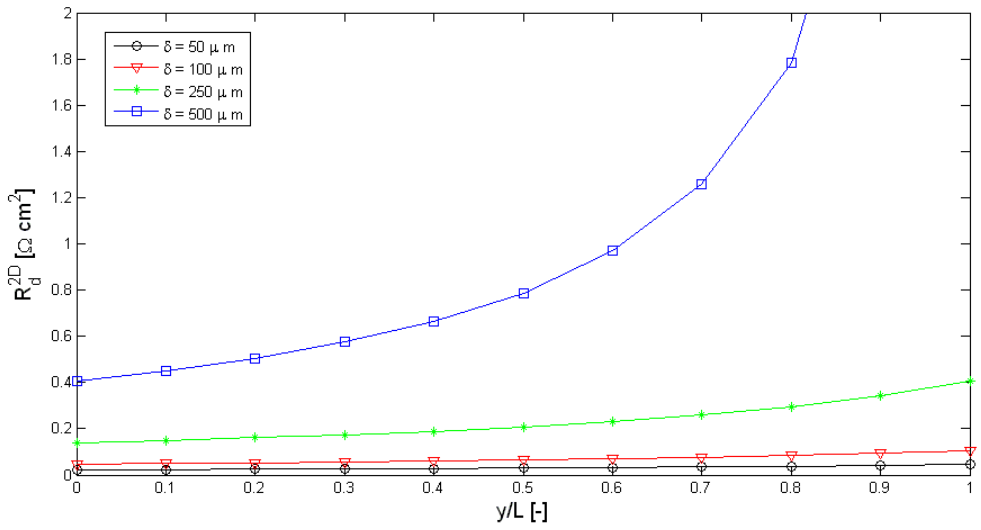

Figure 3. Profiles of $R_d^{2D}(y)$ between the air inlet and the air outlet for different values of the diffusion layer thickness and with an air stoichiometry S_{O2} = 2 (starting from data of *Bultel et al.* (15), table I).

The curves in Figure 3 show that the thickness of the diffusion layer can have a great impact on mass transfer kinetics: when S_{O2} = 2, reducing its initial value (500 µm (15)) by one half decreases significantly the mass transfer limitations ($\Delta R_d^{2D}(L)$ is reduced by a factor of about 14) and the $R_d^{2D}(y)$ profile becomes almost flat. When S_{O2} = 4, $\Delta R_d^{2D}(L)$ depends less on the diffusion layer thickness but $\Delta R_d^{2D}(L)$ is still divided by about two when dividing the diffusion layer thickness also by two.

With relatively simple hypotheses, this alternative expression of the Warburg diffusion impedance shows that in certain conditions, mass transfer limitations due to oxygen consumption along the channel can be quite significant: the usual 1D expression remains satisfying only for large values of the air stoichiometry which do not correspond to usual operating conditions. Further investigations should focus on the time-variations of the oxygen concentration resulting from upstream consumption and convection, which should entail -in some cases- a time-shift between oscillation in current density and in oxygen concentration, as a function of the flow velocity (24).

Identification of the main characteristics of diffusion media

EIS could also be used to estimate the geometrical characteristics of diffusion layers. As $R_d^{1D/2D}$ and τ_d depend both on the diffusion medium thickness δ, on the effective diffusivity D_{eff}, and indirectly on the porosity ε [9], the experimental impedance spectra can be used to identify the value of these parameters. Starting from the expression of the characteristic diffusion time τ_d [27], that of $R_d^{1D/2D}$ [29, 30] and that from the charge transfer resistance R_{tc} [23], one can obtain relations giving the thickness of the diffusion medium. It depends on the operating conditions and on the impedance parameters τ_d and $R_d^{1D/2D}$, which must be determined experimentally:

$$\delta = \frac{\tau_d J}{4Fc_{02}^0}\left(\frac{R_{tc}}{R_d^{1D}}+1\right). \qquad [32]$$

$$\delta = \frac{\left\langle j_f(y)\right\rangle_t \tau_d}{4Fc_{02}^0 \dfrac{IS_{02} - d\int_0^y \left\langle j_f(y)\right\rangle_t dy}{IS_{02}\left(1+H\right)}}\left(\frac{R_{tc}}{R_d^{2D}}+1\right). \qquad [33]$$

Actually, equation [33] expresses δ as a function of y and it is necessary to consider its mean value over the electrode length L. In the absence of other information, assuming a homogeneous current density, $\left\langle j_f\right\rangle_y = I / dL$, it comes:

$$\delta = \frac{J\tau_d}{4Fc_{02}^0 \dfrac{S_{02}-\frac{1}{2}}{S_{02}\left(1+H\right)}}\left(\frac{R_{tc}}{R_d^{2D}}+1\right). \qquad [34]$$

The limiting diffusion layer can be determined by comparing the value of δ identified from the experimental spectra to the actual thickness of the gas diffusion layer and of the active layer. Furthermore, comparing the results of equations [32] and [33], shows whether oxygen transport can be considered as one dimensional or 2-dimensional. Examples of results are presented in the following, using data published by *Rubio et al.* (23), which are obtained with a single PEM cell of S = 100 cm^2 operating at 12.5 A. The fuel cell is fed by pure H_2 and air (at 1 atm) with a stoichiometry S_{O2} = 2.3 (23).

According to *Rubio et al*., the charge transfer resistance R_{tc} = 13.2 mΩ and the diffusion resistance R_d = 7.97 mΩ. Since the cell temperature was not controlled, it has to be estimated, as well as the air inlet relative humidity. Knowing that the fuel cell was not humidified, we chose T_{cell} = 60 °C and RH = 0.1. The identified values for δ and D_{eff} are given in table II.

Table II: Diffusion layer thickness δ and effective diffusion coefficient identified starting from experimental results of Rubio et al. (23) and comparison with typical values from the literature. Oxygen is assumed to diffuse in gas phase in the GDL and the active layer: the possible presence of liquid is accounted through the actual value of the porosity ε.

Model	**δ [m]**	**D_{eff} [m^2 s^{-1}]**	**ε_{GDL}**	**ε_{AL}**
1D	$0.834\ 10^{-3}$	$9.94\ 10^{-7}$	0.18	0.27
pseudo 2D	$1.2\ 10^{-3}$	$1.96\ 10^{-6}$	0.25	0.43
Literature	GDL: $0.42\ 10^{-3}$ [27] AL: $10\ 10^{-3}$ (est.)	GDL: $3.2\ 10^{-5} \times \varepsilon_{GDL}^2$ AL: $6.9\ 10^{-6} \times \varepsilon_{AL}^{3/2}$ (25)	0.2 - 0.6 (5)	0.2 – 0.35 (26)

The differences between values of the diffusion layer thickness δ and of the effective diffusion coefficient D_{eff} obtained with the usual Warburg expression and with the one resulting from the pseudo-2D approach shows clearly that gas consumption along the air channel has a significant influence, at least in these operating conditions. The classical one-dimensional Warburg expression yields a value of the effective diffusion coefficient typical of active layers [table II]; the corresponding value of the porosity (starting from an equivalent -molecular and Knudsen- diffusion coefficient equal to $6.9\ 10^{-6} \times \varepsilon_{AL}^{3/2}$ [9]) is also within the range generally considered for active layers. However, using the finite Warburg impedance, the estimated thickness of the diffusion layer is almost 2 orders of magnitude larger than that of an active layer (≈ 10 µm). As a consequence, the 1D model does not allow conclude about the limiting layer for mass transfer. Using the pseudo-2D approach [34], both the porosity and the equivalent diffusion coefficient are within ranges typical of gas diffusion layers. The estimated thickness is about 3 times larger than actual GDL thickness, which could be explained by gas diffusion in the *y* direction below the channel rib (increasing the total diffusion length) and/or by a possible mass transfer resistance in the gas channel. Thus, the pseudo 2D approach returns results pointing out the gas diffusion layer as the limiting mass transfer layer, in accordance with some previous works (15).

Conclusions and perspectives

EIS is frequently used to investigate the origin of the mass transfer impedance in cathode gas diffusion and active layers. However, the classical expression of a finite Warburg element used for analysing impedance spectra is obtained assuming that the oxygen concentration at the gas channel/gas diffusion layer interface is constant. This hypothesis is much constraining when the gas stoichiometry is low, and it could lead to wrong estimates of mass transfer parameters characterising the diffusion media. An alternative to this expression is proposed: considering gas consumption along the gas channel entails minor changes to the classical Warburg expression but the first numerical applications show that conclusions about the mass transfer limiting layer and its main characteristics can be significantly modified. The estimated value of the GDL thickness is significantly higher than the actual one, which could be linked to a possible mass transfer resistance in the gas channel and/or to constriction effects in the GDL, below the channel rib. Considering oxygen consumption also makes it possible to investigate variations in local impedance spectra and in the diffusion kinetics along the air channel.

These first results are only of qualitative interest and should be shortly confirmed by specific experimental investigations. Other alternatives to the expression of Warburg impedance will also be evaluated, by considering for instance mass transfer resistance in the gas channel or at the interface between the channel and the GDL.

References

1. J. Deseure, *J. Power Sources*, **178**, 323 (2008).
2. E. Passalacqua, G. Squadrito, F. Lufrano, A. Patti and L. Giorgi, *J. Appl. Electrochem.*, **31**, 449 (2001).
3. J. Ihonen, M. Mikkola and G. Lindbergh, *J. Electrochem. Soc.*, **151**, 1152 (2004).
4. T.E. Springer, T.A. Zawodzinski and S. Gottesfeld, *J. Electrochem. Soc.*, **138**, 2334 (1991).
5. T.E. Springer, T.A. Zawodzinski, M.S. Wilson and S. Gottesfeld, *J. Electrochem. Soc.*, **143**, 587 (1996).
6. M. Eikerling and A.A. Kornyshev, *J. Electroanal. Chem.*, **475**, 107 (1999).
7. Y. Bultel, L. Genies, O. Antoine, P. Ozil and R. Durand, *J. Electroanal. Chem.*, **527**, 143 (2002).
8. J.R. Selman and Y.P. Lin, *Electrochim. Acta*, **38**, 2063 (1993).
9. N. Wagner, *J. Appl. Electrochem.*, **32**, 859 (2202).
10. B; Andreaus, A.J. McEvoy and G.G. Scherer, *Electrochim. Acta*, **47**, 2223 (2002).
11. E. Warburg, *Ann. Phys. Chem.*, **67**, 493 (1899).
12. J. Kim, S.-M. Lee, S. Srinivasan and C.E. Chamberlin, *J. Electrochem. Soc.*, **142**, 2670 (1995).
13. S. Srinivasan and H.D. Hurwitz, *Electrochim. Acta*, **12**, 495 (1967).
14. J. Ramousse, J. Deseure, O. Lottin, S.Didierjean and D. Maillet, *J. Power Sources*, **145**, 416 (2005).
15. Y. Bultel, K. Wiezel, F. Jaouen, P. Ozil and G. Lindbergh, *Electrochim. Acta,* **51**, 474 (2005).
16. D. Armost and P. Schneider, *Chem. Eng. J.*, **57**, 91 (1995).
17. M. Boillot, Phd dissertation, INPL-ENSIC, Nancy (2005).
18. G. E. Archie, Trans. AIME **146**, 54-61 (1942).
19. S. Torquato, *Random Heterogeneous Materials: Microstructure and Macroscopic Properties*, Springer (2002).
20. H. C. Bruggeman, Berechnung verschiedener Physikalischer Konstanten von heterogenen Substanzen, *Ann. Physik (Liepzig)* **24,** 636-679 (1935).
21. P. Argyropoulos, K. Scott, W. M. Taama, *J. Appl. Electrochem*. **29,** 661-669 (1999).
22. C. S. Kong, D. Y. Kim, H. K. Lee, Y. G. Shul, T. H. Lee, *J. Pow. Sources* **108,** 185-191 (2002).
23. M.A. Rubio, A.Urquia, R.Kuhn and S.Dormido, *J. Power Sources*, **183**, 118 (2008).
24. I.A. Schneider, S.A. Freunberger, D. Kramer, A. Wokaun and G.G. Scherer, *J. Electrochem. Soc.*, **154**, B770 (2007).
25. R. B. Bird, W. E. Stewart and E. N. Lightfoot, *Transport Phenomena*, p.517, John Wiley and Sons, Inc. (2002).
26. A. Fischer, J. Jindra and H. Wendt, *J. Appl. Electrochem.*, **28**, 277 (1998).
27. Sigracet®, *www.servovision.com/fuel_cell_components/gdl_10.pdf.*